

A precessing molecular jet signaling an obscured, growing supermassive black hole in NGC1377?*

S. Aalto¹, F. Costagliola¹, S. Muller¹, K. Sakamoto², J. S. Gallagher^{3, 1}, K. Dasyra⁴, K. Wada⁵, F. Combes⁶, S. García-Burillo⁷, L. Kristenssen⁸, S. Martín^{9, 10, 11}, P. van der Werf¹², A. S. Evans¹³, and J. Kotilainen¹⁴

(Affiliations can be found after the references)

Received xx; accepted xx

ABSTRACT

With high resolution ($0.''25 \times 0.''18$) ALMA CO 3–2 (345 GHz) observations of the nearby ($D=21$ Mpc, $1''=102$ pc), extremely radio-quiet galaxy NGC1377, we have discovered a high velocity, very collimated nuclear outflow which we interpret as a molecular jet with a projected length of ± 160 pc. The launch region is unresolved and lies inside a radius $r < 10$ pc. Along the jet axis we find strong velocity reversals where the projected velocity swings from -180 km s⁻¹ to $+180$ km s⁻¹. A simple model of a molecular jet precessing around an axis close to the plane of the sky can reproduce the observations. The velocity of the outflowing gas is difficult to constrain due to the precession but we estimate it to be between 250 and 600 km s⁻¹ and the jet to precess with a period $P=0.7$ -1.5 Myr. The CO emission is clumpy along the jet and the total molecular mass in the high velocity gas (± 60 to 180 km s⁻¹) lies between $2 \times 10^6 M_{\odot}$ (light jet) and $2 \times 10^7 M_{\odot}$ (massive jet).

We discuss the driving mechanism of the molecular jet and suggest that it is either driven by a (fading) radio jet or by an accretion disk-wind similar to those found towards protostars. It seems unlikely that a massive jet could have been driven out by the current level of nuclear activity which should then have undergone rapid quenching. The light jet would only have expelled 10% of the nuclear gas and may facilitate nuclear activity instead of suppressing it. The precession can be powered by a binary supermassive black hole (SMBH) or by a flow of gas of misaligned angular momentum onto a warped accretion disk. We find large columns of H₂ in the nucleus of NGC1377 which may be a sign of a high rate of recent gas infall. The nucleus of NGC1377 harbours intense embedded activity and if the current IR luminosity is powered by a growing SMBH it would have an accretion rate of $\sim 10\%$ Eddington. There is tentative evidence that the molecular gas in the jet is decelerating with radius suggesting that the gas in the outflow can return and fuel future nuclear growth. The dynamical age of the molecular jet is 0.3-1 Myr which could imply that it is young and consistent with the notion that NGC1377 is caught in a transient phase of its evolution. However, further studies are required to determine the age of the molecular jet, its mass and the role it is playing in the growth of the nucleus of NGC1377.

There is also a broad, cone-like structure of CO emission in NGC1377 which seems to be a slower, wide-angle molecular outflow. Most of the CO flux in NGC1377 is located here and the estimated mass of the cone is approximately $10^8 M_{\odot}$.

Key words. galaxies: evolution — galaxies: individual: NGC1377 — galaxies: active — galaxies: jets — galaxies: ISM — ISM: molecules

1. Introduction

The growth of central baryonic mass concentrations and their associated supermassive black holes (SMBHs) are key components of galaxy evolution (Kormendy & Ho 2013). The underlying processes behind the evolution of the SMBH and how it is linked to its host galaxy and its interstellar gas are, however, not well understood. In addition, it is not clear how SMBHs can grow despite the energy/luminosity of accretion that leads to gas expulsion from the region. Massive molecular outflows powered by AGNs and bursts of star formation are suggested to be capable of driving out a large fraction of the galaxy's cold gas reservoir in only a few tens of Myr (e.g. Nakai et al. 1987; Walter et al. 2002; Feruglio et al. 2010; Sturm et al. 2011; Aalto et al. 2012a; Combes et al. 2013; Bolatto et al. 2013; Cicone et al. 2014; Sakamoto et al. 2014;

García-Burillo et al. 2014; Aalto et al. 2015b; Alatalo 2015; Feruglio et al. 2015).

Cold molecular gas has been proposed to be an important source of fuel for SMBH growth since accretion of hot gas is suggested to be inefficient and slow (Blandford & Begelman 1999; Nayakshin 2014). However, it is not known how the cold gas is deposited into the inner nucleus of the galaxy. This *angular momentum problem* is similar for the growth of SMBHs and the formation of stars (Larson 2010) and is even more severe for SMBHs because they are smaller than stars in relation to the size of the system in which they form. Thus, the mass SMBHs may achieve is likely strongly regulated by the efficiency of angular momentum transfer during the fuel process. Chaotic inflows of cold gas clumps with randomly oriented angular momenta therefore have been suggested as alternatives to large scale disks in feeding the growth of the SMBH (King & Pringle 2007; Gaspari et al. 2013; Nayakshin et al. 2012). In this scenario SMBH growth may occur primarily through multiple small-scale accretion events - rather than continuous accretion (e.g. King & Pringle 2007) leading to AGN luminosity variations on time scales $10^3 - 10^6$ yr (Hickox et al. 2014). AGN

* Based on observations carried out with the ALMA Interferometer. ALMA is a partnership of ESO (representing its member states), NSF (USA) and NINS (Japan), together with NRC (Canada) and NSC and ASIAA (Taiwan), in cooperation with the Republic of Chile. The Joint ALMA Observatory is operated by ESO, AUI/NRAO and NAOJ.

luminosity thus is expected to vary depending on the interplay between accretion, outflow and winds.

To test how gas inflow and the feedback of central activity influences the growth of SMBHs it is important to study galaxies in early, or transient, phases of their nuclear evolution. NGC1377 is a likely example of such a system. It belongs to a small subset of galaxies that deviates strongly from the well-known radio-to-FIR correlation through having excess FIR emission as compared to the radio ($q > 3$; $q = \log[\text{FIR}/3.75 \times 10^{12} \text{ Hz}]/S_{\nu}(1.4\text{GHz})$ (Helou et al. 1985)). The FIR-excess galaxies are rare - Roussel et al. (2003) find that they represent a small fraction (1%) of an infrared flux-limited sample in the local universe, such as the IRAS Faint Galaxy Sample. Their scarcity is likely an effect of the short time spent in the FIR-excess phase making them ideal targets for studies of transient stages of AGN, starburst and feedback.

1.1. The extremely radio-quiet FIR-excess galaxy NGC 1377

NGC 1377 is a member of the Eridanus galaxy group at an estimated distance of 21 Mpc ($1'' = 102 \text{ pc}$) and has a far-infrared luminosity of $L_{\text{FIR}} = 4.3 \times 10^9 L_{\odot}$ (Roussel et al. 2003). In stellar light, NGC 1377 has the appearance of a regular lenticular galaxy (de Vaucouleurs et al. 1991) although Heisler & Vader (1994) found a faint dust lane extending along the southern part of the minor axis.

NGC 1377 is the most radio-quiet, FIR-excess galaxy known *do date* with radio synchrotron emission being deficient by at least a factor of 37 with respect to normal galaxies (Roussel et al. 2003, 2006). Interestingly, H II regions are not detected through near-infrared hydrogen recombination lines or thermal radio continuum even though faint optical emission lines are present (Roussel et al. 2003, 2006). Deep mid-infrared silicate absorption features suggest that the nucleus is enshrouded by large masses of dust (e.g. Spoon et al. 2007). The compact IR nucleus has been suggested to be the site either of a nascent ($t < 1 \text{ Myr}$) opaque starburst (Roussel et al. 2003, 2006) or of a buried AGN (Imanishi 2006; Imanishi et al. 2009).

High resolution SMA CO 2–1 observations revealed a large central concentration of molecular gas and a massive molecular outflow (Aalto et al. 2012b) that appeared to be young ($\approx 1.4 \text{ Myr}$). The extremely high nuclear dust and gas obscuration of NGC1377 aggravates the determination of the nature of the nuclear activity and the driving force of the molecular outflow, but the extraordinary radio deficiency implies transient nuclear activity.

We used the Atacama Large Millimeter/submillimeter Array (ALMA) to observe CO 3–2 at high resolution in NGC1377 aiming to determine the nature of the buried source and the structure and evolutionary status of the outflow. Here we present the discovery of a high-velocity, extremely collimated and precessing molecular jet in NGC1377. Our results show that the nuclear source is likely an AGN and that we are either witnessing the sudden death of a radio jet that drove a molecular collimated outflow or a jet powered by cold accretion. The nuclear activity of NGC1377 may be fading - or the large nuclear concentration of gas and dust signify that the major AGN event has not occurred yet. We also discuss how the gas transfer in the molecular jet may foster gas recycling and how this process may act as an engine that promotes SMBH growth.

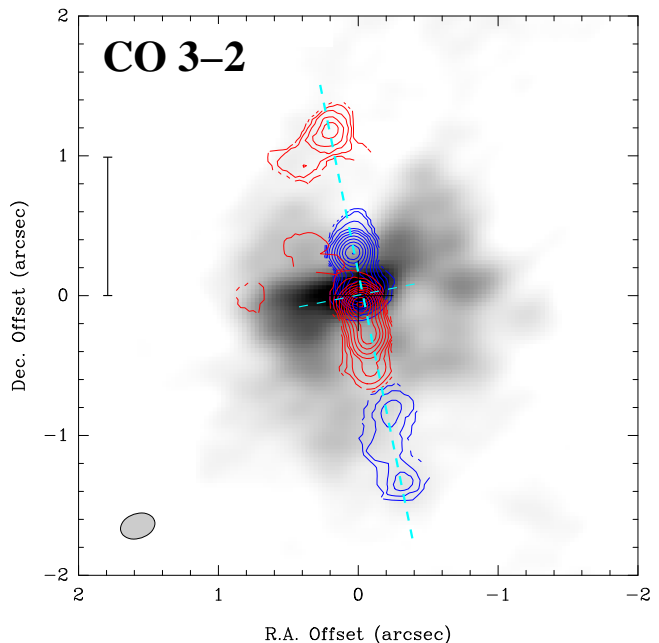


Fig. 2. CO 3–2 integrated intensity image where emission at systemic velocity ($0 \text{ to } \pm 60 \text{ km s}^{-1}$) is shown in gray scale and the high velocity ($\pm 60 \text{ to } \pm 180 \text{ km s}^{-1}$) emission from the molecular jet in red and blue contours (showing the velocity reversals). The dashed lines mark the jet axis and the orientation of the nuclear disk. The CO 3–2 beam is shown as a grey ellipse at the bottom left corner. The vertical bar marks a scale of 100 pc.

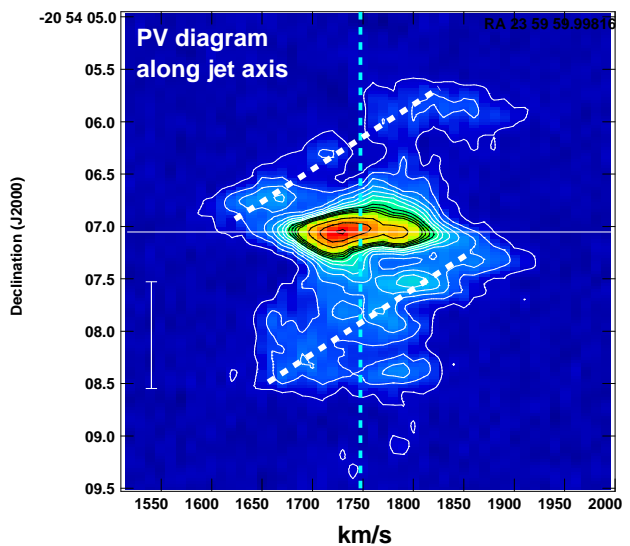


Fig. 3. Position-velocity (PV) diagram showing gas velocities in a slit along the jet axis. The dashed white lines indicate model predictions for precession and outward motion of the molecular jet. Contour levels are $3.1 \times (1, 2, 4, 8, 16, 32) \text{ mJy beam}^{-1}$ thus the first level is at 4σ . The colour scale range from $-11 \text{ to } 156 \text{ mJy beam}^{-1}$.

2. Observations

Observations of the CO J=3–2 line were carried out with ALMA (with 35 antennas in the array) on 2014 August 12th, for about half an hour on-source and with good atmospheric conditions (precipitable amount of water vapor of $\sim 0.5 \text{ mm}$). The phase center was set to $\alpha = 03:36:39.074$ and $\delta = -20:54:07.055$ (J2000).

The correlator was set up to cover two bands of 1.875 GHz in spectral mode, one centered at a frequency of $\sim 344.0 \text{ GHz}$

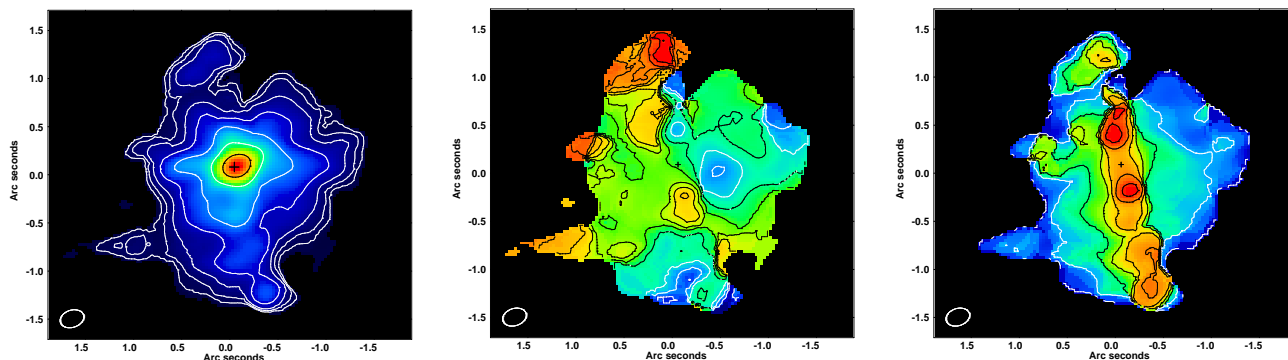


Fig. 1. CO 3-2 moment maps. Left: Integrated intensity (mom0) where contours are $1.7 \times (1, 2, 4, 8, 16, 32, 64)$ Jy km s⁻¹ beam⁻¹. Colours range from 0 to 172 Jy km s⁻¹ beam⁻¹. Centre: velocity field (mom1) where contours range from 1690 km s⁻¹ to 1820 km s⁻¹ in steps of 10 km s⁻¹. Right: Dispersion map (mom2) where contours are $4.4 \times (1, 3, 5, 7, 9, 11, 13)$ km s⁻¹ and the jet is clearly seen. Colours range from 0 to 66 km s⁻¹. The cross marks the position of the 345 GHz continuum peak (see Tab. 1).

to cover the CO J=3–2 line (in the lower side band) and the other centered at 354.3 GHz to cover the HCO⁺ J=4–3 and HCN $J = 4 - 3 \nu = 0$ and $\nu = 1f$ lines (in the upper side band). The velocity resolution for these bands was 1.0 km/s after Hanning smoothing. In addition, two 2 GHz bands were set up in continuum mode, i.e., with a coarser velocity resolution of ~ 27 km s⁻¹, centered at 342.2 and 356 GHz, respectively.

The bandpass of the individual antennas was derived from the quasar J0423–0120. The quasar J0340–2119 (~ 0.3 Jy) was observed regularly for complex gain calibration. The absolute flux scale was calibrated using the quasar J0334–401. The flux density for J0334–401 was extracted from the ALMA flux-calibrator database.

After calibration within the CASA reduction package, the visibility set was imported into the AIPS package for further imaging. The synthesized beam is $0.''25 \times 0.''18$ (25×18 pc for NGC1377) with Briggs weighting (parameter robust set to 0.5) and the resulting data has a sensitivity of 0.8 mJy per beam in a 10 km s⁻¹ (12 MHz) channel width.

3. Results

The CO 3–2 integrated intensity (moment 0) map, velocity field (moment 1) and dispersion map (moment 2) are presented in Fig 1. The moment 0 maps shows a peak at the continuum nucleus and multiple structures that are apparently protruding radially from the center. The velocity field is complex and shows that the maximum velocity shifts are occurring outside the nucleus. *The moment 2 map reveals a striking structure where the highest dispersion outlines a collimated jet feature originating from the nuclear region inside a radius $r < 10$ pc.* The width of the jet is set by our beam resolution.

3.1. The molecular jet

The high velocity (projected velocities 60–180 km s⁻¹) gas (Fig. 2) is aligned in a $\pm 1.''5$ (± 160 pc) long jet-like feature with strong velocity reversals along the jet axis. Near the nucleus (within $0.''1$) the highest redshifted velocity is on the southern side and the highest blueshifted velocities to the north. Further along the jet axis (within $0.''5$) this reverses. The jet is highly collimated with an unresolved width ($d < 20$ pc) and a position angle PA=10°. The position velocity (PV) diagram (Fig. 3) shows the velocity reversals clearly along the jet axis. It also shows that the maximum velocities occur about $0.''2$ (20 pc) away from the

Table 1. CO 3–2 flux densities and molecular masses^a

Position ^b (J2000)	α : 03:36:39.073 ($\pm 0.''01$) δ : -20:54:07.05 ($\pm 0.''01$)
Peak flux density ^c	270 ± 16 (mJy beam ⁻¹)
Flux	
(central beam)	17.4 ± 0.05 (Jy km s ⁻¹ beam ⁻¹)
(molecular jet) ^d	23.2 ± 0.5 (Jy km s ⁻¹)
(whole map)	159 ± 0.5 (Jy km s ⁻¹)
Molecular mass ^e	
(central beam)	$1.8 \times 10^7 M_{\odot}$
(molecular jet)	$2.3 \times 10^7 M_{\odot}$
(whole map)	$16 \times 10^7 M_{\odot}$

a) Listed errors are 1σ rms.

b) The position of the peak CO 3–2 integrated intensity. The peak T_B is at α :03:36:39.072 δ :-20:54:07.06 at $V_c=1730$ km s⁻¹.

c) The Jy to K conversion in the $0.''25 \times 0.''18$ beam is 1 K=4.6 mJy. The peak T_B is 34 K corresponding to 156 mJy.

d) The jet flux is integrated from $\pm(60$ to $200)$ km s⁻¹ where the blueshifted flux is 5.5 and the redshifted 17.7 Jy km s⁻¹.

e) The H₂ mass $M(H_2)=1 \times 10^4 S(CO1-0)\Delta\nu D^2$ (D is the distance in Mpc, $S\Delta\nu$ is the integrated CO 1–0 line flux in Jy km s⁻¹) for a conversion factor $N(H_2)/I(CO 1-0)=2.5 \times 10^{20}$ cm⁻²). Since we have CO 3–2 we have to correct for the frequency dependence of the brightness temperature conversion. If CO 3–2 and 1–0 have the same brightness temperature (thermal excitation, optically thick) the correction factor is 1/9. However, usually the CO emission is subthermally excited and the brightness temperature ratio is expected to be about 0.5 for a giant molecular cloud. Hence the correction factor we apply is 1/4.5 and $M(H_2)=2.2 \times 10^3 S(CO 3-2)\Delta\nu D^2$. The inferred H₂ column density in the central beam is $N(H_2)=3 \times 10^{24}$ cm⁻².

nucleus. The CO emission along the jet axis is clumpy, but the clumps are unresolved in the CO 3–2 beam. From the Jy to K conversion in Tab. 1 we find that the clumps have brightness temperatures $T_B(CO 3-2)=1 - 8$ K. The CO 3–2 line widths of the gas clumps in the jet are high ranging from 50 to ~ 150 km s⁻¹

which is evident in the PV diagram along the jet axis - but also in PV diagrams cut across the jet (Fig 6).

3.2. Systemic- and low velocity gas

The systemic and low velocity gas is outlining a cone-like feature surrounding the molecular high velocity jet (Fig. 2 in grayscale). Most of the CO 3–2 flux of NGC1377 is emerging from this structure (Tab. 1). The extent of the systemic emission is similar to that of the high velocity molecular jet, but we note that at zero velocities negatives in the map indicate that there is some missing flux from extended emission. The maximum recoverable scale of our observations is of the order of $\sim 5''$.

3.3. Nuclear gas and continuum

Velocities in the nucleus span a total of 250 km s^{-1} . It is not clear which fraction of this constitutes rotation of a circumnuclear disk and which fraction stems from the jet (or the cone). From the CO luminosity we infer an H_2 column density of $N(\text{H}_2)=3 \times 10^{24} \text{ cm}^{-2}$ (Tab. 1) towards the nucleus. This would imply that the nucleus of NGC1377 is Compton thick - similar to the nuclei of other extremely obscured early type disk galaxies such as NGC4418 (Sakamoto et al. 2013; Costagliola et al. 2013), IC860 and Zw049.057 (Falstad et al. 2015; Aalto et al. 2015a), but more studies are required to confirm this high $N(\text{H}_2)$ for NGC1377.

Apart from CO 3–2 we also detected HCO^+ and H^{13}CN $J = 4 - 3$, vibrationally excited HCN $J = 4 - 3$ $\nu_2 = 1f$ ($T = E_1/k=1050 \text{ K}$) and vibrationally excited HC_3N $J = 38 - 37$ $\nu_4 = 1$, $\nu_7 = 1$ ($T = E_1/k=1891 \text{ K}$). The vibrationally excited lines are factor 20-30 times fainter than CO 3–2 in the nucleus, but their detection is consistent with a large $N(\text{H}_2)$ and the presence of very hot gas and dust (Aalto et al. 2015a).

The 342 GHz continuum consists of a compact component and some extended emission. In the $0.''25 \times 0.''18$ beam the deconvolved FWHM size is $0.''25 \times 0.''09$ and a position angle $\text{PA}=105 \pm 10^\circ$. The continuum is faint ($1.3 \pm 0.1 \text{ mJy beam}^{-1}$ and $2.2 \pm 0.3 \text{ mJy}$ integrated). We assume that the continuum peaks on the nucleus of the galaxy.

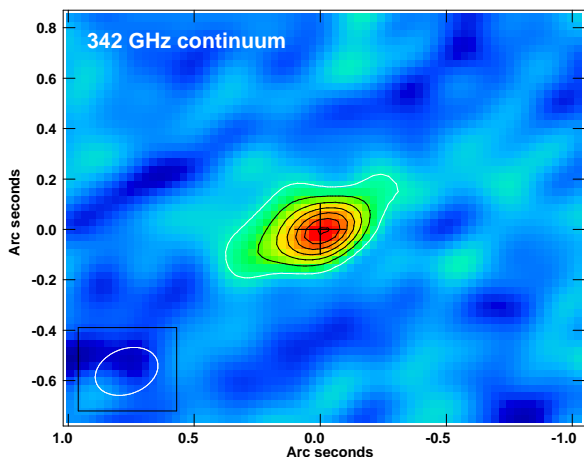


Fig. 4. 342 GHz continuum. Contour levels are $0.19 \times (1,2,3,4,5,6,7)$ mJy beam^{-1} . The cross marks the continuum peak position

4. Discussion

4.1. The origin of the high velocity gas

4.1.1. A precessing molecular jet

We interpret the high velocity gas detected in CO 3–2 as a highly collimated and ordered molecular jet. *The striking velocity reversals we observe along the jet are consistent with those of jet precession* (see e.g. (Rosen & Smith 2004)).

In Fig 3 we see that the velocity swings from $+180 \text{ km s}^{-1}$ to -180 km s^{-1} along the jet, suggesting that its axis should be relatively close to the plane of the sky and that it is launched from a highly inclined disk. The 342 GHz continuum image (Fig. 4) implies a nuclear disk of inclination $70^\circ \pm 10^\circ$ - and a FWHM radius of 13 pc. (Although we caution that the continuum emission is faint and only marginally resolved.)

In Fig. 5 we present a simple model of a molecular jet with a precession angle of 20° and an inclination of the precession axis close to zero. The resulting outflow velocity depends on which velocity contour of Fig. 3 we select. The 4σ contours of the first turn (at $0.''2$) gives $v_{\text{out}}=530 \text{ km s}^{-1}$ while a fit to the FWHM velocities gives $v_{\text{out}}=250 \text{ km s}^{-1}$. In the first case the precession period is $P=0.7 \text{ Myr}$ and for the slower outflow $P=1.5 \text{ Myr}$. The precession angle is not well constrained and may be smaller - leading to higher v_{out} . We conclude that the outflow velocity lies between 250 and 600 km s^{-1} . This is higher than the estimated bulge escape velocity for NGC1377 (Aalto et al. 2012b).

The molecular jet emerges from the nucleus and its width is unresolved resulting in a launch region of the jet inside $r=10 \text{ pc}$. The nuclear rotation is unresolved but from the PV diagram we estimate a rotational velocity of $\approx 110 \text{ km s}^{-1}$ and if this occurs at $r=10 \text{ pc}$ the rotational timescale is $\sim 1 \text{ Myr}$. The precession period must be longer than the rotational time scale of the jet launching region and hence the jet is very likely launched close

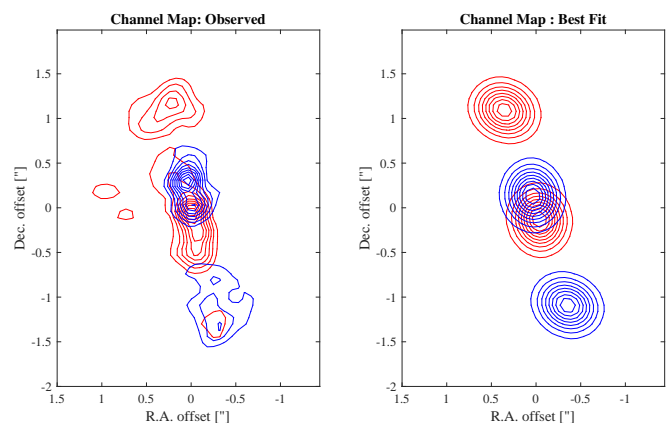


Fig. 5. Contour plots of integrated red- and blueshifted emission (>66 and $<66 \text{ km s}^{-1}$) for ALMA data (right) and model of precessing jet (left). The precession angle is 20° and the inclination of the model precession axis along the line of sight is close to zero.

4.1.2. Origin of the jet precession

Jet precession may be caused by a warped accretion disk (Greenhill et al. 2003) - i.e. by the misalignment between the spin orientation of the black hole and the surrounding accretion

disk (Lu & Zhou 2005) and an accretion flow transporting in gas of misaligned angular momentum (Krolik & Hawley 2015).

Alternatively, in a SMBH binary system, jet precession may be caused by geodetic precession of the spin axis of the primary rotating SMBH being misaligned with the binary total angular momentum - or by inner disk precession (due to the tidal interaction of an inclined secondary SMBH). Orbital periods for these types of precession range between $10^3 - 10^8$ yr and the period should shorten as the two SMBHs grow closer (Komossa 2006; Liu & Chen 2007). Interestingly, the presence of a nuclear gas and dust concentration and a precessing molecular jet can aid the coalescence of the SMBHs into one overcoming the "final-parsec problem" (Milosavljević & Merritt 2003; Aly et al. 2015). The central region of NGC1377 has a post-starburst optical spectrum (Gallager et al in prep.) suggesting the presence of an aging (≈ 1 Gyr) starburst. It is possible that this declining burst of star formation can be linked to a merger event that has now lost all its dynamical signatures and left an SMBH binary in the heart of NGC1377.

4.1.3. Other explanations

An orbiting object? Velocity variations in a PV diagram may also be caused by a jet launched from an orbiting object. In this case the velocity reversals can be dominated by the orbital motion in a near edge-on plane of rotation. A possibility would be a jet launched from one of two orbiting SMBHs. However, without jet precession the velocity pattern will not fit the structure we see in the observed PV diagram. Both SMBHs could have jets and a combination of orientation and length of the jets could probably be put together to reproduce the observed PV diagram. However, this seems unlikely compared to the relatively simple scenario of one single precessing jet.

A bicone projection? We argue that the outflow of NGC1377 consists of (at least) two components: a wide biconic wind (Fig 2 and Sec. 3.2) - and a precessing molecular jet. Is it however possible that our observations can be explained solely by a bicone and that the collimated, high velocity structure is only a projection effect? A tilted biconical outflow could result in projected, foreshortened blueshifted emission from the lower end of the cone - and redshifted (more elongated) emission from the back side of the cone (and vice versa on the underside of the cone). Position velocity (PV) diagrams of these scenarios are presented by (e.g.) Das et al. (2005) and Storchi-Bergmann et al. (2010). To explain the blueshifted emission north of the nucleus the top cone must therefore be tilted towards the observer.

However, In Fig. 6 we show two PV diagrams across the molecular jet in the north and south (offset $\pm 0.''3$). They clearly show that the collimated structure cannot be explained as a bicone projection effect. The spatially unresolved molecular jet clearly stands out as a separate structure from the wide angle gas. We also see that the wide angle gas is slightly more redshifted to the north compared to that in the south (by ≈ 50 km s^{-1}).

4.2. Comparing to previous results on NGC1377

In our previous paper on NGC1377 (Aalto et al. 2012b) we suggested that the molecular outflow seen in CO 2-1 is biconic with an opening angle of $60^\circ - 70^\circ$, an outflow mass $> 1 \times 10^7 M_\odot$ and an outflow velocity of 140 km s^{-1} . These observations were carried out with three times poorer spatial resolution and about ten times lower flux sensitivity than the ALMA CO 3-2 data presented here. The CO 2-1 dispersion map has a cross-like struc-

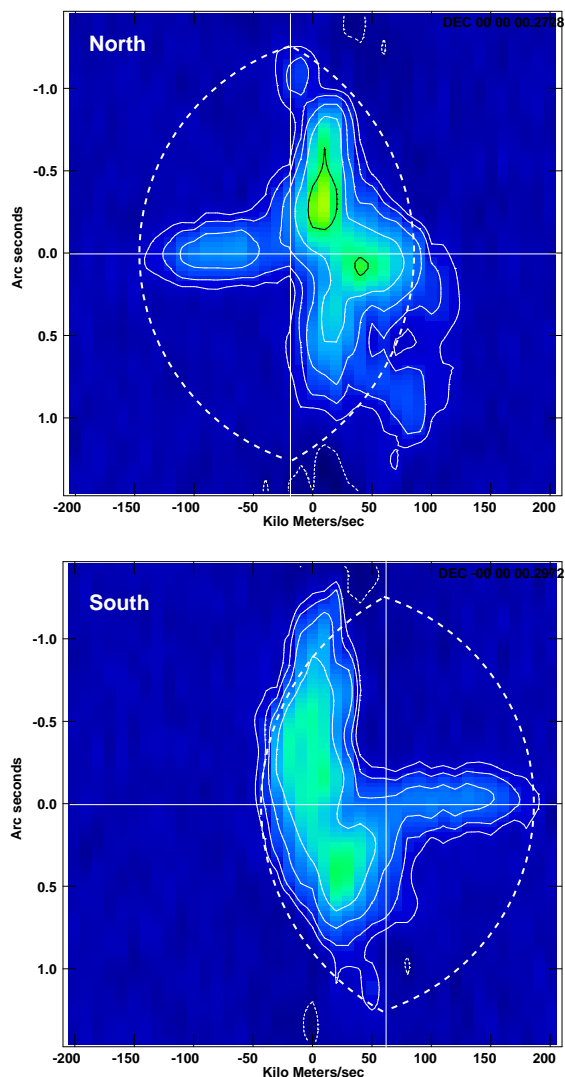


Fig. 6. Position-velocity (PV) diagram showing gas velocities in a slit across the jet axis at $\pm 0.''3$. Contour levels are $3.1 \times (1, 2, 4, 8, 16, 32)$ mJy beam^{-1} . The colour scale ranges from -11 to 156 mJy beam^{-1} . The dashed semi-ellipticals show the PV diagram expected from a projected wide-angle cone as described in Sec. 4.1.3. we see here that this model does not fit the data.

ture that we used as a base to suggest the biconic outflow. In the ALMA data, high dispersion is found only along a structure that we now identify as a molecular jet.

It is interesting to note that the position angle of the outflow in the lower resolution CO 2-1 map is around $PA=40^\circ$ while the CO 3-2 jet has a PA of 10° . The differences between the CO 3-2 and 2-1 maps may be a result of resolution and sensitivity only, but it is also possible that the lower resolution SMA map is picking up a different component of the outflowing gas. We speculate that this may be due to the jet precession or that it is the remnant of previous jet-activity by a second SMBH in a potential binary. Further studies hopefully will reveal the origin of this gas component

It is also interesting to compare the CO outflow signatures with the optical dust absorption feature south of the nucleus visible in Fig. 1 in Roussel et al. (2006). V-shaped and jet-like dusty features extend out to 2 kpc from the nucleus. Their age is roughly 10 Myr (for $v_{\text{out}}=200$ km s^{-1}) and may be remnants of a previous outflow event in NGC1377.

4.3. Mass and outflow rate

The molecular mass in the high velocity gas is estimated to $M_j(\text{H}_2) = 2.3 \times 10^7 M_\odot$ assuming a standard CO to H_2 conversion factor (see Tab. 1). For a projected length of the outflow of 160 pc and an outflow velocity of 530 km s^{-1} the age of the outflow is 0.8 Myr and the mass outflow rate is $25 M_\odot \text{ yr}^{-1}$. Given that the outflow velocity lies between 250 and 600 km s^{-1} we estimate the mass outflow rate to $9 - 30 M_\odot \text{ yr}^{-1}$. This results in a momentum flux of $(14 - 112)L/c$ which is very high and typically seen in cases of AGN feedback (Cicone et al. 2014; García-Burillo et al. 2014). However, since we use a standard conversion factor, the H_2 mass may have been overestimated. If the gas is turbulent and the individual gas clouds unbound the conversion factor may have to be adjusted down by a factor of 10 (Dahmen et al. 1998). The line widths are indeed broad in the molecular jet of NGC1377 (Sec. 3.1), but this does not necessarily reflect the internal velocity dispersion of individual clumps in the jet, but may be an effect of the precession/projection. The imprint of the disk rotation will also be carried out with the jet.

The *total* molecular mass in the NGC1377 outflow should also include the gas in the wide-angle cone. The CO luminosity in the cone is significantly higher than that in the jet and the total outflowing molecular mass can be very high in NGC1377. The relation between the jet and the cone will be discussed in a future paper.

A remarkable feature of NGC1377 is that the bulk of the CO 3–2 emission resides in the outflow component and not in the molecular disk.

4.4. What is powering the molecular jet?

4.4.1. Accretion

Jets are generally identified with accretion (Blandford 1998; Konigl & Pudritz 2000; Hujeirat et al. 2003; Sbarrato et al. 2014) and are likely launched by magnetohydrodynamic processes from the accretion disk and/or the central object. For the molecular jet of NGC1377 we discuss two main scenarios: A. entrainment by a radio jet and B. cold accretion.

The molecular mass is a crucial ingredient in determining the energetics, nature and evolutionary stage of the molecular jet. We have to resort to a CO to $M(\text{H}_2)$ conversion factor to determine the molecular mass and we have two limiting cases: A *massive jet* where $M_j(\text{H}_2) \sim 10^7 M_\odot$ or a *light jet* with $M_j(\text{H}_2) \sim 10^6 M_\odot$. Below we discuss the two driving scenarios in relation to a massive or a light jet:

A. Entrainment by a radio jet

Powerful radio jets are launched when a SMBH is growing through *hot accretion* which is an inefficient accretion at low rates (<1% Eddington) (McAlpine et al. 2015). This is also referred to as *radio mode* AGN feedback. Radio jet production has been found for high Eddington rates where the jet powers do not exceed the bolometric luminosity of their AGNs (Sikora et al. 2013). The jet may entrain molecular gas from the disk of the host galaxy (NGC1266 (Alatalo et al. 2011), IC5063 (Morganti et al. 2015), M51 (Matsushita et al. 2007) and NGC1068 (García-Burillo et al. 2014)) or the molecular gas may form in the jet itself through rapid post-shock cooling (Morganti et al. 2015). The molecular gas distribution associated with these jets tends to be patchier than the more coherent molecular structure of NGC1377. A relativistic radio jet ploughing through a thick disk of gas, is likely to heat and ionise it around, and thus forming a wide cocoon of multi-phase and tur-

bulent gas mixture, as simulated by Wagner & Bicknell (2011)). As shown in Dasyra et al. (2015) such a cocoon is both pushing on the surrounding gas and has front- and backward internal flows that may lead to a complicated velocity pattern. Although it is not clear how this model could explain the highly ordered jet motions in NGC1377, including a jet-ISM interaction in the form of a cocoon is likely important for a full understanding of the gas motions in the radio-jet scenario

However, NGC1377 is the most radio-quiet (with respect to the IR luminosity) galaxy found so far and its radio power is very low. We can use the limit to the 1.4 GHz radio luminosity (Roussel et al. 2006) and the relation between jet power and 1.4 GHz luminosity (Bîrzan et al. 2008) to obtain a limit on the energy in a potential radio jet in NGC1377. We find that it amounts to <10% of the mechanical energy in the massive molecular jet. However, it is possible that a short burst of hot accretion in the nucleus led to the formation of a radio jet that then faded very rapidly without re-acceleration of electrons in the jet itself. If the synchrotron life time is $t_s = 8 \times 10^8 B^{-2} \gamma^{-1}$ (where $B=B$ -field, γ =Lorentz factor, (Xu et al. 2000)) a reasonable combination of B and γ can result in a jet life-time of 0.5-1 Myr. Also, it is conceivable that heavily mass-loading a radio jet with dense molecular gas may lead to quenching of the non-thermal radio emission. In the case of the light jet it is feasible that there would be enough radio power to carry out the gas (for the lowest possible v_{out}) without invoking a fading of the radio jet. High resolution imaging will reveal if there is indeed a faint radio jet in NGC1377 - or if the radio emission has a different morphology.

B. Cold gas accretion

The jet may be a hydromagnetic disk-wind or an accretion X-wind similar to the extremely collimated molecular outflows found in accreting low-mass protostars (Konigl & Pudritz 2000; Codella et al. 2014; Kristensen 2015). Its torque could efficiently extract disk angular momentum and gravitational potential energy from the molecular gas. The jet may be powered by accretion onto the central object and/or infalling gas onto the nuclear disk. The molecular jet of NGC1377 is highly collimated and very thin - less than 20 pc across. It appears to be the first case of a precessing molecular jet found in an external galaxy - and it is without an obvious radio counterpart. Thus there are no similar objects to compare with - although the double molecular, collimated bipolar outflows found in the luminous merger NGC3256 (Sakamoto et al. 2014) may also be radio faint.

Assuming that the $5 \times 10^9 L_\odot$ of NGC1377 emerges from a growing SMBH, the accretion rate would be $\approx 10^{-3} - 10^{-2} M_\odot \text{ yr}^{-1}$ ($L = \epsilon \dot{M} / dt c^2$ where $\epsilon = 0.1$ onto a $10^6 M_\odot$ SMBH). This is 10% of the inferred Eddington luminosity of the SMBH (Aalto et al. 2012b) and is a relatively high rate placing it in the *quasar mode* of accretion (McAlpine et al. 2015). But it may require an Eddington or super-Eddington accretion rate to produce the mass outflow rate we see even in the case of the light jet. Thus, this scenario would require that the level of SMBH accretion has dropped recently.

A jet may also be powered by accretion onto a nuclear disk. The disk wind model involves the gradual collimation of a centrifugally driven wind from a magnetized accretion disk. The wind energy is derived from the gravitational energy released from the disk through gas rotation and a coupled magnetic field. In this case the extracted angular momentum allows cold molecular gas to sink further towards the nucleus. In the case of the massive jet M_j is similar to that in the disk inside its launching region M_d . The binding energy of jet is similar to the binding energy of the disk and the outflow speed is at least twice that of

the rotational velocity (unless the jet is actually launched very close to the nucleus from a Keplerian disk). It is not clear how the current rotational energy could continue to sustain the outflow of the massive jet. In the case of the light jet the binding energy of the jet would be much less than that of the disk and there would be enough rotational energy to sustain the outflow.

The molecular jet is observed to be lumpy which may be due to internal shocks - or the condensations are gas clumps originating in separate accretion/outflow events. If so, the energetics of the outflow may be different from that of the steady flow scenario we assume above.

4.4.2. Other scenarios

Radiation pressure from dust? Recent work by Ishibashi & Fabian (2015) suggests that large momentum flux outflows ($> 10L/c$) can be obtained in radiation pressure driven outflows if radiation trapping is taken into account. However, it is not clear how radiation pressure would result in a jet-like feature since it should give rise to a more wide-angle wind.

Starburst winds? In Aalto et al. (2012b) we discuss the faintness of the star formation tracers (such as optical, NIR and radio emission) of NGC1377. We find that the upper limits on, for example, the 1.4 GHz continuum imply that star formation falls short by at least one order of magnitude in explaining the momentum flux in the molecular outflow detected with the SMA. Radio continuum emission has remained undetected in NGC1377 until recently when 1.5 and 9 GHz emission was found with the Jansky Very Large Array (JVLA) (Costagliola et al. in prep.). The emission is very faint and its spectral index suggests synchrotron- rather than thermal free-free emission from HII regions. With the new 1.4 GHz flux we find that supernovae emission is too faint by a factor of 50 to drive the outflow. We find no evidence of an embedded nascent pre-supernova starburst. In addition, the high degree of collimation and strong precession of the molecular jet also imply that it is not powered by the winds of an embedded stellar cluster.

4.5. Is the molecular jet signalling nuclear growth or quenching?

There is large molecular mass in the nucleus of NGC1377 which is powering a current SMBH accretion at a respectable rate of $\sim 10\%$ Eddington. So the question is - has the molecular jet action quenched the nuclear activity - or did it promote it?

In Sec. 4.4.1 we suggest two scenarios for powering the molecular jet: A. entrainment by a radio jet and B. cold accretion onto a SMBH and/or disk-accretion. We also discuss two limiting mass loss cases: the massive jet where the jet and nuclear disk mass are comparable - and the light jet where $M_d \gg M_j$.

Light jet: Both scenarios A. and B. could power the jet and may promote SMBH accretion. This is because the jet has removed only 10% of the disk mass while it may have transported a substantial amount of angular momentum away from the gas in the disk enabling it to sink to the SMBH.

In this context it is interesting to consider the potential relation to cold chaotic accretion. Nayakshin et al. (2012) suggest that SMBHs grow through the chaotic accretion of gas clouds with small and randomly distributed angular momentum. They argue that "planar mode" of feeding - i.e. that a large scale disk is connected to (and feeding) a nuclear disk around a SMBH - is not an important mode of SMBH growth since such disks are

unstable to gravitational fragmentation and star formation which interrupts the gas flows. The molecular jet of NGC1377 offers a way for the cold gas to shed itself of excess angular momentum, enabling nuclear accretion without the requirement that the accreting gas clouds have randomly oriented angular momenta. In addition, there appears to be a mechanism that prevents stars from forming even in high gas surface density disks since the nucleus of NGC1377 has a very low star formation rate that has yet to reach the SMBH.

Massive jet: Current rates of accretion would have difficulty explaining a large mass outflow rate. Nuclear activity in the form of radio luminosity, or other forms of accretion luminosities, are low and perhaps are a signature of quenching. The turning off of the nuclear activity would have to have been abrupt since the molecular jet can be traced all the way down to the nucleus. Furthermore, the large masses of molecular gas are surprising since it is not clear why the activity would turn off with 30% of the nuclear fuel still in place. A possible explanation could be that there has been a recent substantial inflow of molecular gas.

4.5.1. Is the jet part of a feeding "engine"?

There is not much gas in the rotating disk of NGC1377 - instead most of it ($> 10^8 M_\odot$) appears to be in the slowly moving cone and about 1% - 20% of that in the molecular jet. The gas along the jet appears to slow down and it has not (so far) reached further than 150- 200 pc away from the nucleus. There seems to be no fast moving gas outside of $2''$ - 200 pc above the nucleus and it is possible that its outward motion dissipates in the jet. Hence the gas in the outflow may be set to fall back onto NGC1377 where it may participate in another cycle of nuclear growth. In this scenario the outflow with subsequent returning gas functions as an engine of nuclear growth. Even if only 10% of the total cone+jet gas returns and ends up accreting onto the SMBH its mass will be above that expected from the $M - \sigma$ relation.

The molecular jet appears to be a young structure with a dynamical age of 0.3 to 1 Myr (depending on v_{out}). The outflow may be a recent outburst within an older structure through which the nucleus of NGC1377 goes through cyclic growth. Alternatively, the molecular gas is not slowing down and falling back, but instead becomes dissociated at 200 pc and continues outward in the form of ionized gas. Deep multi-wavelength observations of the outflow of NGC1377 are necessary to address the issue of the age and fate of the gas in the molecular jet.

5. Conclusions

With high resolution ($0.''2 \times 0.''18$) ALMA CO 3-2 observations of the nearby extremely radio-quiet galaxy NGC1377, we have discovered a high velocity, collimated molecular jet. We find strong evidence that the jet is precessing around an axis close to the plane of the sky with a gas outflow velocity between 250 and 600 km s^{-1} . The jet precession may be powered by a binary SMBH or by accretion of gas with misaligned angular momentum onto a warped nuclear disk. The jet is launched close to the nucleus inside a radius $r < 10$ pc. There is also a broad, cone-like structure of CO emission in NGC1377 which may be a slower, wide-angle molecular outflow. Most of the CO flux in NGC1377 is located here and the estimated mass of the cone is $\approx 10^8 M_\odot$. The jet molecular mass lies between 2×10^6 (*light jet*) and $2 \times 10^7 M_\odot$ (*massive jet*) depending on which CO to $M(\text{H}_2)$ conversion factor is adopted.

We discuss potential powering mechanisms for the molecular jet. It may be gas entrained by a radio jet or driven by an accretion disk-wind similar to those found in protostars. It is important to better constrain the jet molecular mass. Given the possibility of either a light or a heavy jet it is difficult to draw conclusions on whether the jet is quenching the nuclear activity - or instead is enabling it. The light jet would only have driven out 10% of the nuclear gas and should not be quenching the activity. It seems unlikely that a massive jet could have been driven out by the current activity and this may be a sign of rapid quenching. In this case the large mass of H₂ in the nucleus is surprising and may be caused by a recent massive influx of gas. Even though the gas in the molecular jet has a high outflow velocity there are some tentative signs that it is slowing down. If so, the gas may return to the inner region of NGC1377 to fuel further nuclear growth; the nucleus may have been recently refuelled with gas stemming from previous cycles of activity.

NGC1377 is the first galaxy where a precessing, highly collimated molecular jet has been found. The extreme q -value for NGC1377 and the short apparent time-scale of the molecular jet (0.3 - 1 Myr) are signs consistent with the notion that we see NGC1377 in a transient phase of its evolution. We speculate that a merger event left a binary SMBH which is now driving the evolution of the nuclear region of NGC1377. Alternatively, in-falling misaligned gas tilts the axis of the accretion disk. In either case, NGC1377 offers a unique opportunity for detailed studies of the processes that feed, promote and quench nuclear activity in galaxies. Further studies are required to determine the age of the molecular jet, its mass and the role it is playing in the growth of the nucleus of NGC1377.

Acknowledgements. This paper makes use of the following ALMA data: ADS/JAO.ALMA#2012.1.00900.S. ALMA is a partnership of ESO (representing its member states), NSF (USA) and NINS (Japan), together with NRC (Canada) and NSC and ASIAA (Taiwan), in cooperation with the Republic of Chile. The Joint ALMA Observatory is operated by ESO, AUI/NRAO and NAOJ. We thank the Nordic ALMA ARC node for excellent support. SA acknowledges partial support from the Swedish National Science Council grant 621-2011-4143. KS was supported by grant MOST 102-2119-M-001-011-MY3 SGB thanks support from Spanish grant AYA2012-32295. JSG thanks the Chalmers University for the appointment of *Jubileumsprofessor* for 2015. SA thanks Sabine König and Åke Hjalmarson for discussions of the manuscript.

References

- Aalto, S., Costagliola, S. M. F., Gonzalez-Alfonso, E., et al. 2015a, ArXiv e-prints [arXiv:1504.06824]
- Aalto, S., Garcia-Burillo, S., Muller, S., et al. 2015b, A&A, 574, A85
- Aalto, S., Garcia-Burillo, S., Muller, S., et al. 2012a, A&A, 537, A44
- Aalto, S., Muller, S., Sakamoto, K., et al. 2012b, A&A, 546, A68
- Alatalo, K. 2015, ApJ, 801, L17
- Alatalo, K., Blitz, L., Young, L. M., et al. 2011, ApJ, 735, 88
- Aly, H., Dehnen, W., Nixon, C., & King, A. 2015, MNRAS, 449, 65
- Birzan, L., McNamara, B. R., Nulsen, P. E. J., Carilli, C. L., & Wise, M. W. 2008, ApJ, 686, 859
- Blandford, R. D. 1998, in American Institute of Physics Conference Series, Vol. 431, American Institute of Physics Conference Series, ed. S. S. Holt & T. R. Kallman, 43–52
- Blandford, R. D. & Begelman, M. C. 1999, MNRAS, 303, L1
- Bolatto, A. D., Warren, S. R., Leroy, A. K., et al. 2013, Nature, 499, 450
- Cicone, C., Maiolino, R., Sturm, E., et al. 2014, A&A, 562, A21
- Codella, C., Cabrit, S., Gueth, F., et al. 2014, A&A, 568, L5
- Combes, F., Garcia-Burillo, S., Casasola, V., et al. 2013, A&A, 558, A124
- Costagliola, F., Aalto, S., Sakamoto, K., et al. 2013, A&A, 556, A66
- Dahmen, G., Huttemeister, S., Wilson, T. L., & Mauersberger, R. 1998, A&A, 331, 959
- Das, V., Crenshaw, D. M., Hutchings, J. B., et al. 2005, AJ, 130, 945
- Dasyra, K. M., Bostrom, A. C., Combes, F., & Vlahakis, N. 2015, ArXiv e-prints [arXiv:1503.05484]

- de Vaucouleurs, G., de Vaucouleurs, A., Corwin, Jr., H. G., et al. 1991, Third Reference Catalogue of Bright Galaxies, ed. de Vaucouleurs, G., de Vaucouleurs, A., Corwin, H. G., Jr., Buta, R. J., Paturel, G., & Fouque, P.
- Falstad, N., González-Alfonso, E., Aalto, S., et al. 2015, A&A, 580, A52
- Feruglio, C., Fiore, F., Carniani, S., et al. 2015, ArXiv e-prints [arXiv:1503.01481]
- Feruglio, C., Maiolino, R., Piconcelli, E., et al. 2010, A&A, 518, L155+
- García-Burillo, S., Combes, F., Usero, A., et al. 2014, A&A, 567, A125
- Gaspari, M., Ruszkowski, M., & Oh, S. P. 2013, MNRAS, 432, 3401
- Greenhill, L. J., Booth, R. S., Ellingsen, S. P., et al. 2003, ApJ, 590, 162
- Heisler, C. A. & Vader, J. P. 1994, AJ, 107, 35
- Helou, G., Soifer, B. T., & Rowan-Robinson, M. 1985, ApJ, 298, L7
- Hickox, R. C., Mullaney, J. R., Alexander, D. M., et al. 2014, ApJ, 782, 9
- Hujeirat, A., Livio, M., Camenzind, M., & Burkert, A. 2003, A&A, 408, 415
- Imanishi, M. 2006, AJ, 131, 2406
- Imanishi, M., Nakanishi, K., Tamura, Y., & Peng, C. 2009, AJ, 137, 3581
- Ishibashi, W. & Fabian, A. C. 2015, MNRAS, 451, 93
- King, A. R. & Pringle, J. E. 2007, MNRAS, 377, L25
- Komossa, S. 2006, Mem. Soc. Astron. Italiana, 77, 733
- Konigl, A. & Pudritz, R. E. 2000, Protostars and Planets IV, 759
- Komendy, J. & Ho, L. C. 2013, ARA&A, 51, 511
- Kristensen, L. E. 2015, IAU General Assembly, 22, 57263
- Krolik, J. H. & Hawley, J. F. 2015, ApJ, 806, 141
- Larson, R. B. 2010, Reports on Progress in Physics, 73, 014901
- Liu, F. K. & Chen, X. 2007, ApJ, 671, 1272
- Lu, J.-F. & Zhou, B.-Y. 2005, ApJ, 635, L17
- Matsushita, S., Muller, S., & Lim, J. 2007, A&A, 468, L49
- McAlpine, K., Prandoni, I., Jarvis, M., et al. 2015, Advancing Astrophysics with the Square Kilometre Array (AASKA14), 83
- Milosavljević, M. & Merritt, D. 2003, ApJ, 596, 860
- Morganti, R., Oosterloo, T., Oonk, J. B. R., Frieswijk, W., & Tadhunter, C. 2015, A&A, 580, A1
- Nakai, N., Hayashi, M., Handa, T., et al. 1987, PASJ, 39, 685
- Nayakshin, S. 2014, MNRAS, 437, 2404
- Nayakshin, S., Power, C., & King, A. R. 2012, ApJ, 753, 15
- Rosen, A. & Smith, M. D. 2004, MNRAS, 347, 1097
- Roussel, H., Helou, G., Beck, R., et al. 2003, ApJ, 593, 733
- Roussel, H., Helou, G., Smith, J. D., et al. 2006, ApJ, 646, 841
- Sakamoto, K., Aalto, S., Combes, F., Evans, A., & Peck, A. 2014, ApJ, 797, 90
- Sakamoto, K., Aalto, S., Costagliola, F., et al. 2013, ApJ, 764, 42
- Sbarrato, T., Padovani, P., & Ghisellini, G. 2014, MNRAS, 445, 81
- Sikora, M., Stasińska, G., Kozłowski-Wierzbowska, D., Madejski, G. M., & Asari, N. V. 2013, ApJ, 765, 62
- Spoon, H. W. W., Marshall, J. A., Houck, J. R., et al. 2007, ApJ, 654, L49
- Storchi-Bergmann, T., Lopes, R. D. S., McGregor, P. J., et al. 2010, MNRAS, 402, 819
- Sturm, E., González-Alfonso, E., Veilleux, S., et al. 2011, ApJ, 733, L16+
- Wagner, A. Y. & Bicknell, G. V. 2011, ApJ, 728, 29
- Walter, F., Weiss, A., & Scoville, N. 2002, ApJ, 580, L21
- Xu, C., Baum, S. A., O’Dea, C. P., Wrobel, J. M., & Condon, J. J. 2000, AJ, 120, 2950

- 1 Department of Earth and Space Sciences, Chalmers University of Technology, Onsala Observatory, SE-439 94 Onsala, Sweden
e-mail: saalto@chalmers.se
- 2 Institute of Astronomy and Astrophysics, Academia Sinica, PO Box 23-141, 10617 Taipei, Taiwan
- 3 Department of Astronomy, University of Wisconsin-Madison, 5534 Sterling, 475 North Charter Street, Madison WI 53706, USA
- 4 Department of Astrophysics, Astronomy & Mechanics, Faculty of Physics, University of Athens, Panepistimiopolis Zografos 15784, Greece
- 5 Kagoshima University, Kagoshima 890-0065, Japan
- 6 Observatoire de Paris, LERMA (CNRS:UMR8112), 61 Av. de l’Observatoire, 75014 Paris, France
- 7 Observatorio Astronómico Nacional (OAN)-Observatorio de Madrid, Alfonso XII 3, 28014-Madrid, Spain
- 8 Harvard-Smithsonian Center for Astrophysics, 60 Garden Street, Cambridge, MA 02138, USA
- 9 European Southern Observatory, Alonso de Córdova 3107, Vitacura, Santiago, Chile
- 10 Joint ALMA Observatory, Alonso de Córdova 3107, Vitacura, Santiago, Chile
- 11 Institut de Radio Astronomie Millimétrique (IRAM), 300 rue de la Piscine, Domaine Universitaire de Grenoble, 38406 St. Martin d’Hères, France
- 12 Leiden Observatory, Leiden University, 2300 RA, Leiden, The Netherlands
- 13 University of Virginia, Charlottesville, VA 22904, USA, NRAO, 520 Edgemont Road, Charlottesville, VA 22903, USA
- 14 Finnish Centre for Astronomy with ESO (FINCA), University of Turku, Väisälantie 20, FI-21500 Kaarina, Finland